Supplementary Information (SI) for Dalton Transactions.
This journal is © The Royal Society of Chemistry 2025

Supporting Information

Tunable Optical Properties in $(110)_p$-oriented Layered Halide Perovskite $FA_4Pb_2I_{7.5}(SCN)_{0.5}$ by Br Substitution

Koki Matsushima[a,b], Takuya Ohmi[b,c,d], Wataru Taniguchi[b], Shoya Nagano[b], Tomoya Fukui[e,f], Takanori Fukushima[e,f], Muhammmad Awais[d], Makhsud Saidaminov[d], Masaki Azuma[b,f,g], and Takafumi Yamamoto *[a,b]

[a.] *Department of Chemistry, Graduate School of Science, Kyoto university, Kitashirakawa Oiwake-cho, Sakyoku, Kyoto, 606-8502, Japan.*

[b.] *Materials and Structures Laboratory, Institute of Integrated Research, Institute of Science Tokyo, 4259 Nagatsuta-cho, Midori-ku, Yokohama, Kanagawa, 226-8501, Japan.*

[c.] *Advanced Phosphor Group, Research Center for Electric and Optical Materials, National Institute for Material Science (NIMS), 1-1, Namiki, Tsukuba 305-0044, Japan.*

[d.] *Department of Electrical & Computer Engineering, University of Victoria, 3800 Finnerty Road, Victoria, British Columbia V8P 5C2, Canada.*

[e.] *Laboratory for Chemistry and Life Science, Institute of Innovative Research, Institute of Science Tokyo, 4259 Nagatsuta-cho, Midori-ku, Yokohama, Kanagawa 226-8501, Japan.*

[f.] *Research Center for Autonomous Systems Materialogy (ASMat), Institute of Integrated Research, Institute of Science Tokyo, 4259 Nagatsuta-cho, Midori-ku, Yokohama, Kanagawa, 226-8501, Japan.*

[g.] *Kanagawa Institute of Industrial Science and Technology, 705-1 Shimoimaizumi, Ebina 243-0435, Japan*

Supplementary Note 1

Characterization of $FA_4Pb_2(Br,SCN)_8$ single crystal

We synthesized a fully Br-substituted $FA_4Pb_2I_{7.5}(SCN)_{0.5}$ single crystal to clarify its structure. The single crystals were obtained by the solid-state reaction method under FA^+ and SCN^- excess conditions as reported in $FA_4Pb_2I_{7.5}(SCN)_{0.5}$.[1] After heating, the sample was a paste that separated into white and light yellowish-green layers in the glass tube (**Figure S3**a). The obtained crystals were picked up from the paste into the Fluorolube® oil because of their air sensitivity. The crystal was plate-shaped with $0.1 \times 0.04 \times 0.03$ mm^3 sizes. The crystals showed green PL emission by exposing blue light (**Figure S4**), but collection of the spectroscopic data was difficult due to the instability.

The single crystal X-ray analysis of the data at 293(2) K revealed that the compound has a monoclinic structure (Space group: $P2_1/c$) with a = 6.0372(3) Å, b = 25.564(2) Å, c = 8.6039(8) Å, and β = 94.902(6)°. Details of crystallographic information are shown in Supporting information (**Tables S4-8**). The determined crystal structure (**Figure S2)** is a $(110)_p$-oriented layered perovskite structure (**Figure 1**).

Although the structure is similar to $FA_4Pb_2I_{7.5}(SCN)_{0.5}$, the crystal symmetry is reduced from orthorhombic *Cmmm* to monoclinic $P2_1/c$ by Br substitution. The size difference between I^- and Br^- may induce this symmetry reduction. The atomic ratio of Br02/S02 = 0.951(7)/ 0.049(7) and Br04/S04 = 0.954(8)/ 0.046(8) at the octahedral terminate site was obtained from single crystal analysis, leading the chemical composition of $FA_4Pb_2Br_{7.81(3)}(SCN)_{0.19(3)}$. This sulfur ratio value is slightly smaller than the iodide counterpart (I/S = 0.857(7)/0.143(7)).[1] We note that the $(110)_p$-oriented layered perovskites $FA_4Pb_2Br_8$ (FA_2PbBr_4) without SCN^- was previously synthesized by solution method.[2] The crystal structures of these compounds are reported with different cell symmetry and lattice parameters at 100 K; triclinic phase of P-1 with a = 8.5642(17) Å; b = 11.884(2) Å; c = 14.312(3) Å, α = 65.92°; β = 73.01°; γ = 83.76° and monoclinic phase of $P2_1/c$ with a = 13.1313(9) Å; b = 7.9763(6) Å; c = 11.7972(8); β = 91.52°.[2] Therefore, the obtained single crystals in this report indeed include SCN^- in the structure.

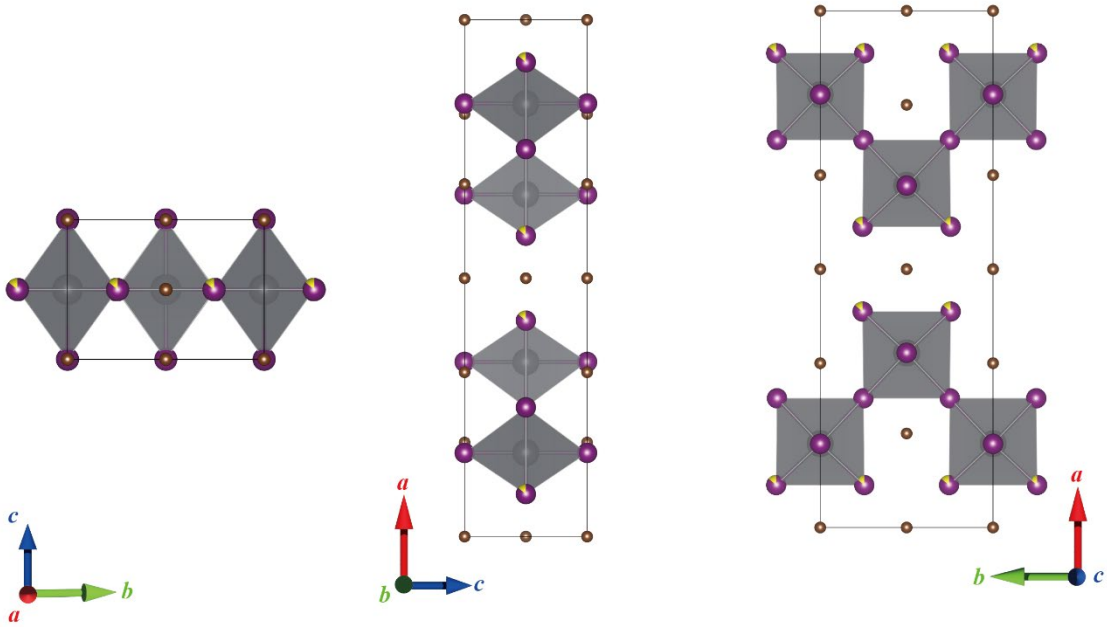


Figure S1. Crystal structure of $FA_4Pb_2I_{7.5}(SCN)_{0.5}$ with *Cmmm*, reported in the reference.[1]

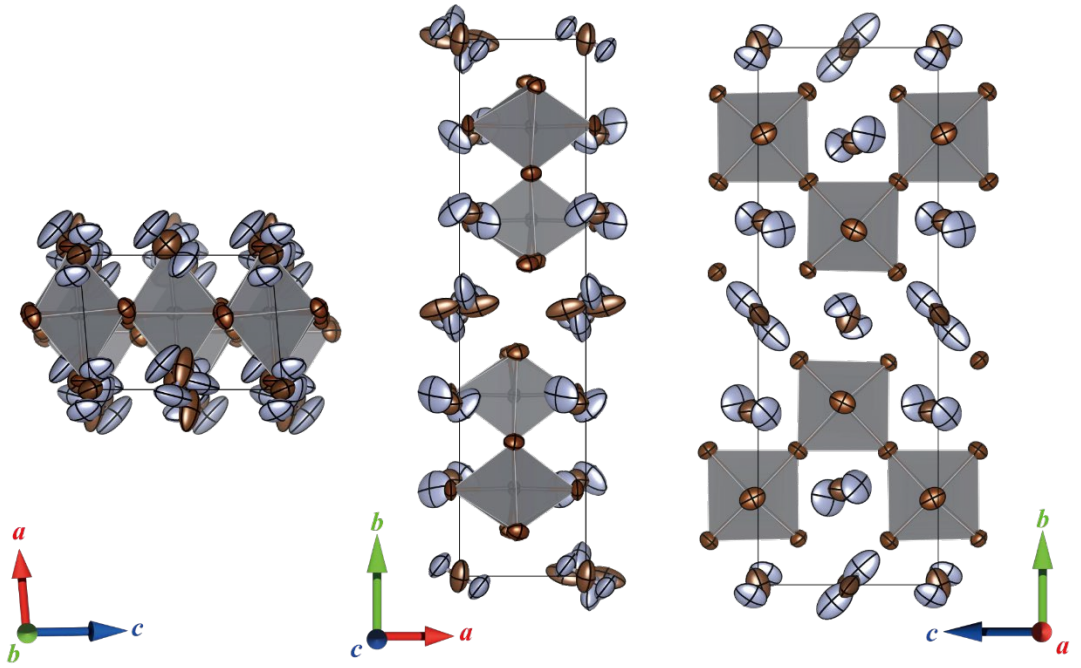


Figure S2. Crystal structure of $FA_4Pb_2Br_{7.81(3)}(SCN)_{0.19(3)}$ with $P2_1/c$, obtained from single crystal XRD. The ellipsoids correspond to 50% probability thermal ellipsoids derived from anisotropic displacement parameters.

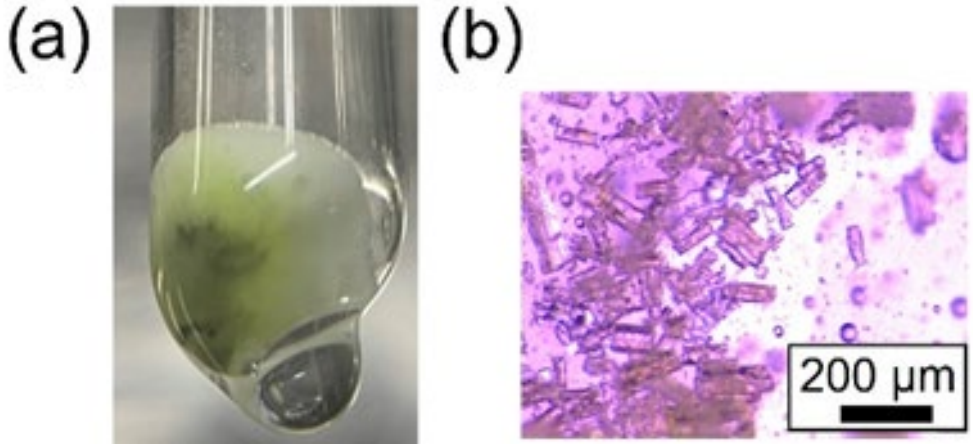


Figure S3. (a) Photograph of the product sealed in a glass tube after heating. (b) Microscopic image of obtained single crystals.

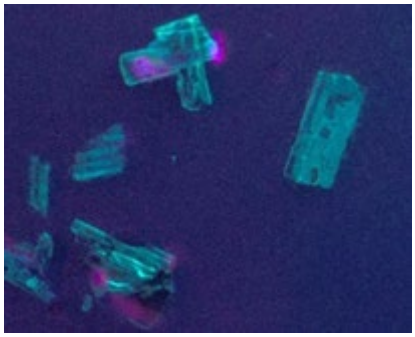


Figure S4. Photograph of the single crystals under UV irradiation.

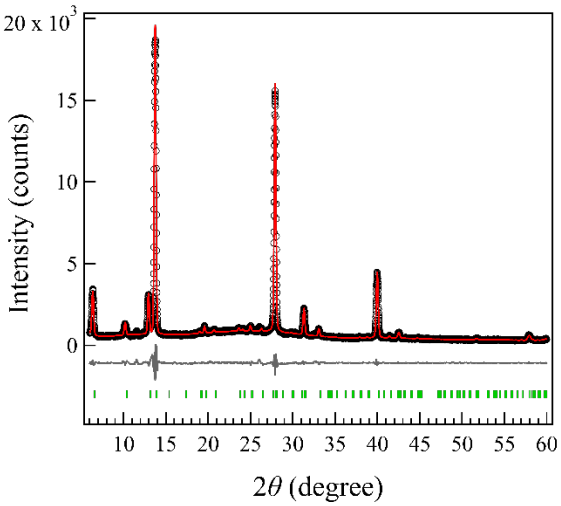


Figure S5. Le Bail refinement result of $x = 0$ at 300 K. Black marks, red line, and gray line represent observed, calculated, and different, respectively, and green ticks show peak positions. GOF, R_{wp}, R_p are 1.80, 4.64%, and 6.30%, respectively.

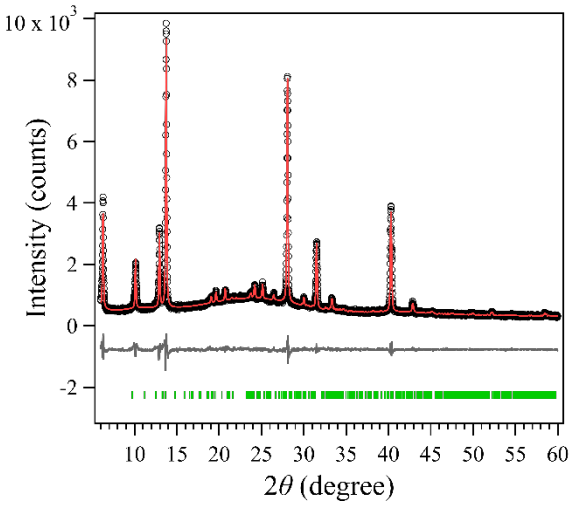


Figure S6. Le Bail refinement result of $x = 0.25$ at 300 K. Black marks, red line, and gray line represent observed, calculated, and different, respectively, and green ticks show peak positions. GOF, R_{wp}, R_p are 1.60, 6.18%, and 4.61%, respectively.

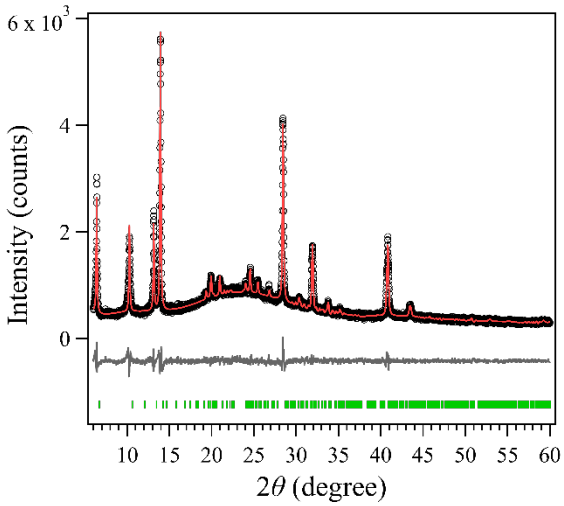


Figure S7. Le Bail refinement result of x = 0.5 at 300 K. Black marks, red line, and gray line represent observed, calculated, and different, respectively, and green ticks show peak positions. GOF, R_{wp}, R_p are 1.46, 5.96%, and 4.53%, respectively.

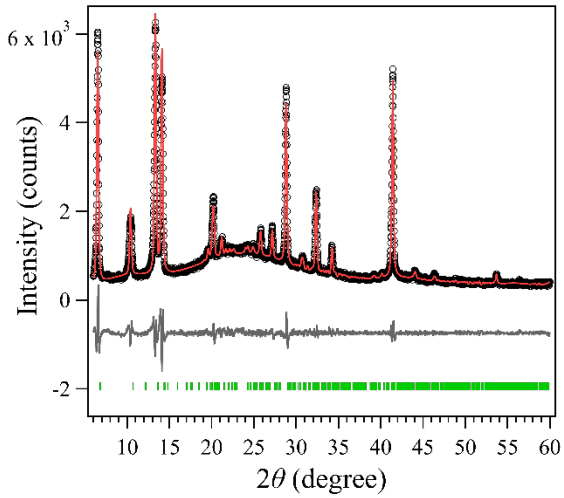


Figure S8. Le Bail refinement result of x = 0.75 at 300 K. Black marks, red line, and gray line represent observed, calculated, and different, respectively, and green ticks show peak positions. GOF, R_{wp}, R_p are 1.99, 7.06%, and 5.23%, respectively.

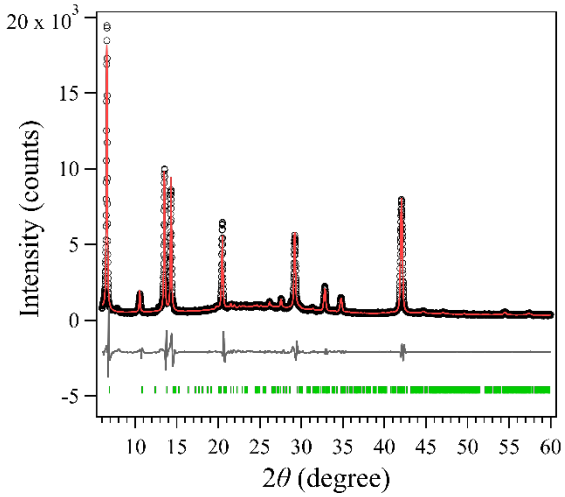


Figure S9. Le Bail refinement result of $x = 1$ at 300 K. Black marks, red line, and gray line represent observed, calculated, and different, respectively, and green ticks show peak positions. GOF, R_{wp}, R_p are 2.80, 9.72%, and 6.93%, respectively.

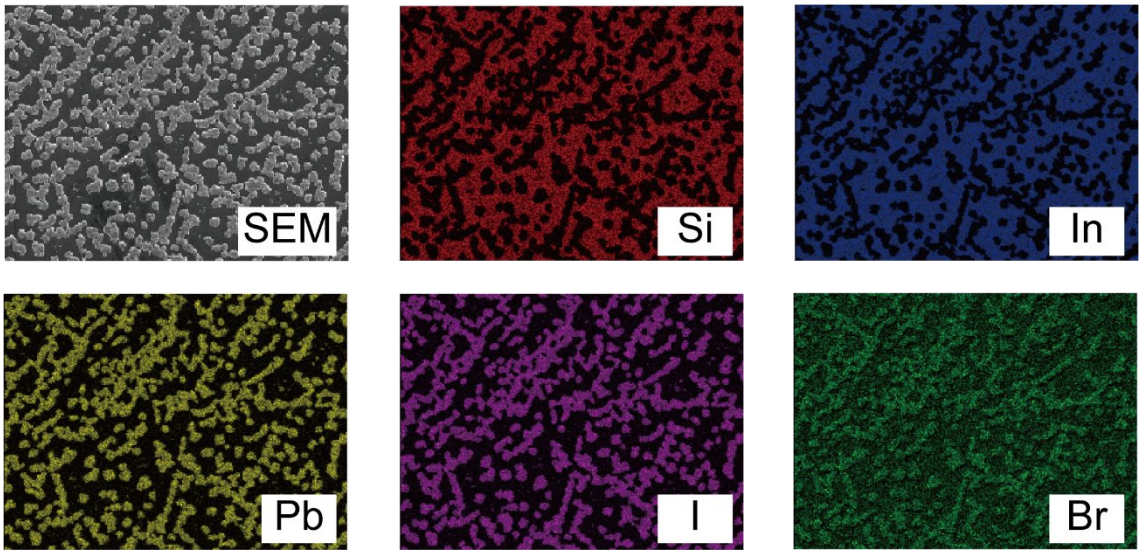


Figure S10. SEM image and EDX mapping of $x = 0.25$ thin film on ITO substrate.

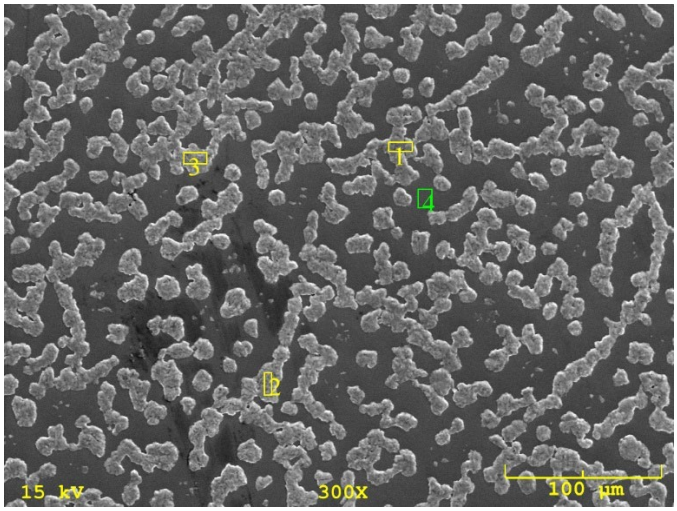


Figure S11. SEM image of $x = 0.25$ thin film on ITO substrate.

Table S1. Atomic concentration at four spots shown in **Figure S11**.

Element	at. %				
	1	2	3	4 (substrate)	Average between 1 to 3
Si	18.0	13.7	18.9	32.8	-
In	33.4	24.9	40.7	59.5	-
Pb	9.7	12.9	8.1	0.8	10.2
I	27.3	35.8	22.2	1.0	28.4
Br	11.6	12.7	10.1	6.0	11.5

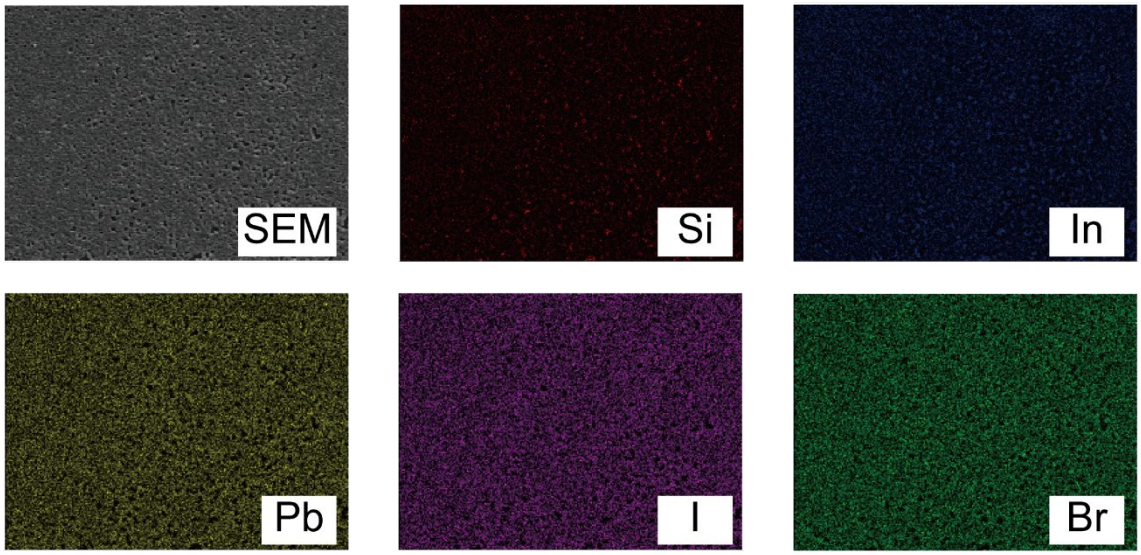


Figure S12. SEM image and EDX mapping of $x = 0.5$ thin film on ITO substrate.

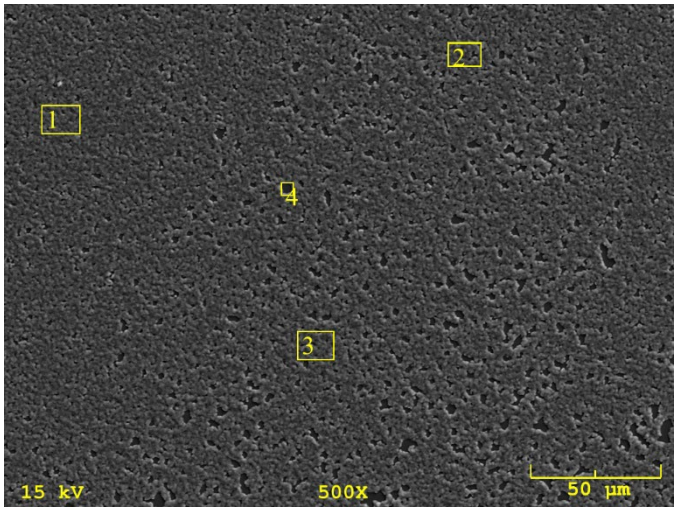


Figure S13. SEM image of $x = 0.5$ thin film on ITO substrate.

Table S2. Atomic concentration at four spots shown in **Figure S13**.

Element	at. %				
	1	2	3	4 (substrate)	Average between 1 to 3
Si	7.9	8.0	7.1	22.3	-
In	29.3	31.7	28.0	54.8	-
Pb	12.9	12.3	13.3	4.4	12.8
I	23.9	23.3	25.2	6.4	24.1
Br	26.1	24.8	26.4	12.2	25.8

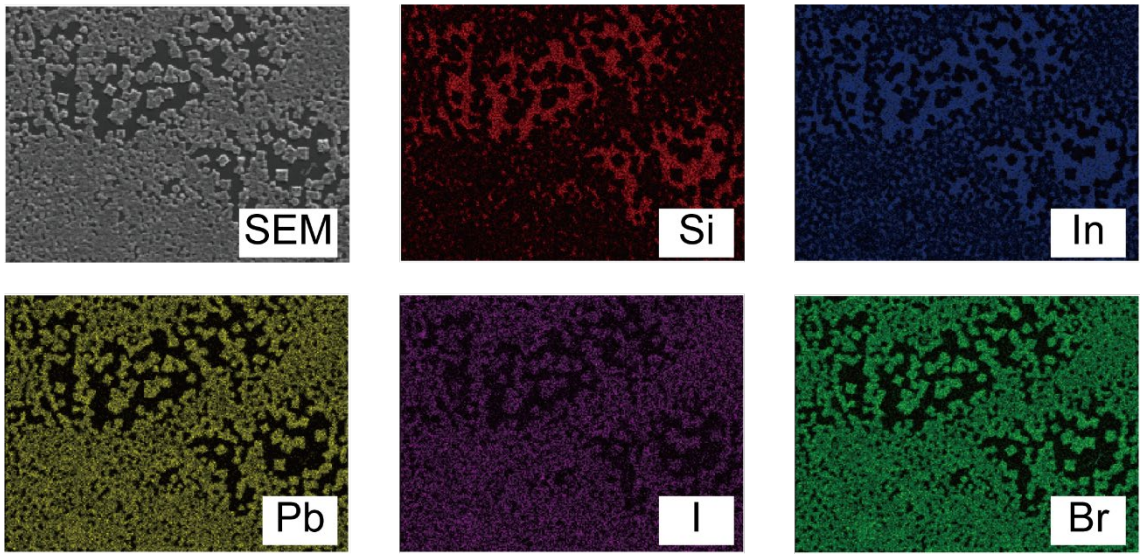


Figure S14. SEM image and EDX mapping of $x = 0.75$ thin film on ITO substrate.

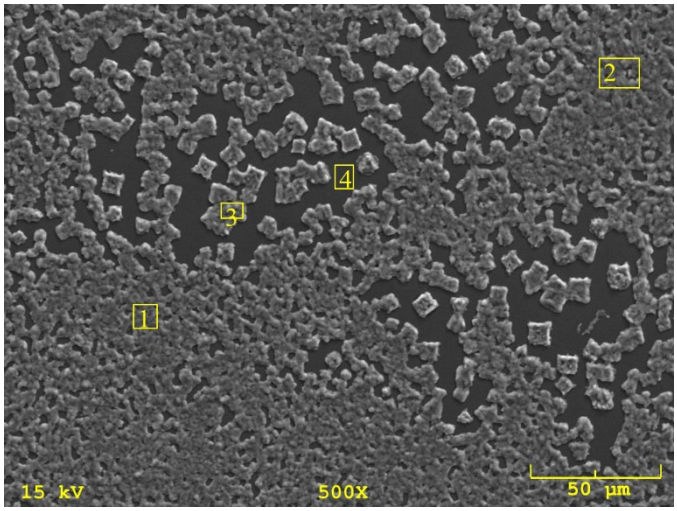


Figure S15. SEM image of $x = 0.5$ thin film on ITO substrate.

Table S3. Atomic concentration at four spots shown in **Figure S13**.

Element	at. %				
	1	2	3	4 (substrate)	Average between 1 to 3
Si	5.3	4.7	1.7	35.3	-
In	25.7	25.2	14.7	58.7	-
Pb	14.8	15.4	18.7	0.1	16.3
I	12.4	13.4	14.9	0.0	13.6
Br	41.8	41.3	50.0	5.9	44.4

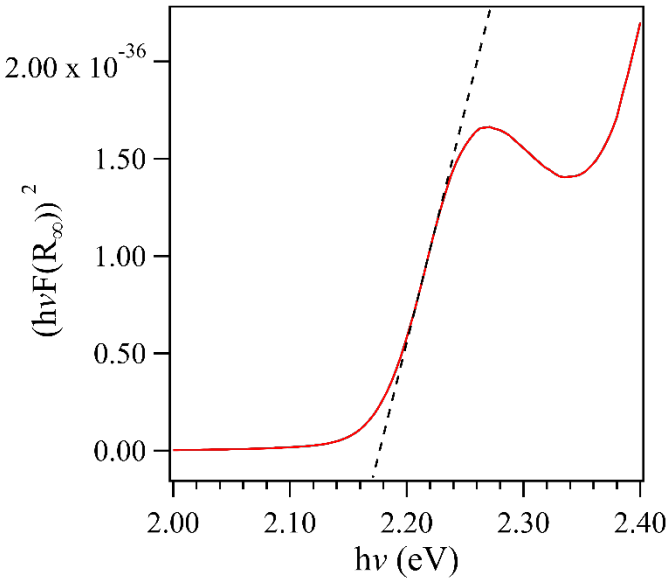


Figure S16. The Tauc's plot of $FA_4Pb_2I_{7.5}(SCN)_{0.5}$ ($x = 0$). Band gap is estimated to 2.18 eV.

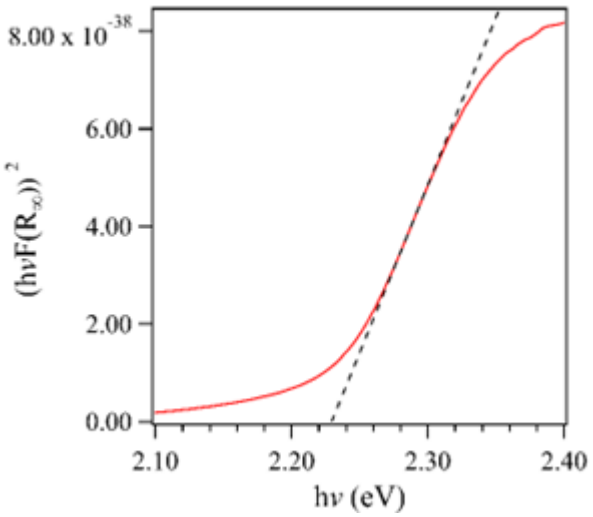


Figure S17. The Tauc's plot of $FA_4Pb_2(Br_{0.25}I_{0.75})_{7.5}(SCN)_{0.5}$ ($x = 0.25$). Band gap is estimated to 2.22 eV.

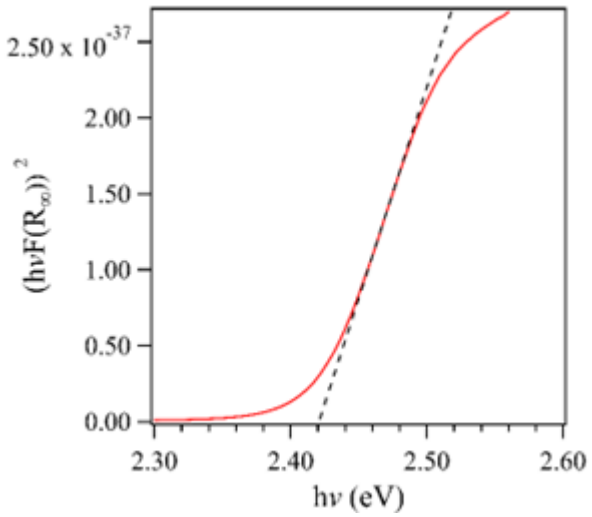


Figure S18. The Tauc's plot of $FA_4Pb_2(Br_{0.5}I_{0.5})_{7.5}(SCN)_{0.5}$ (x = 0.5). Band gap is estimated to 2.42 eV.

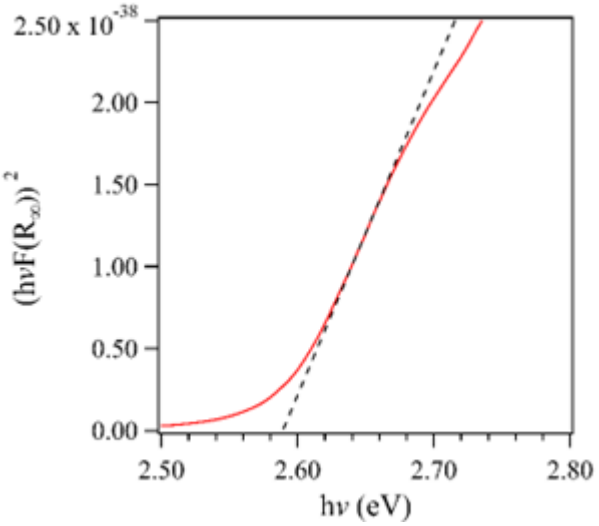


Figure S19. The Tauc's plot of $FA_4Pb_2(Br_{0.75}I_{0.25})_{7.5}(SCN)_{0.5}$ (x = 0.75). Band gap is estimated to 2.59 eV.

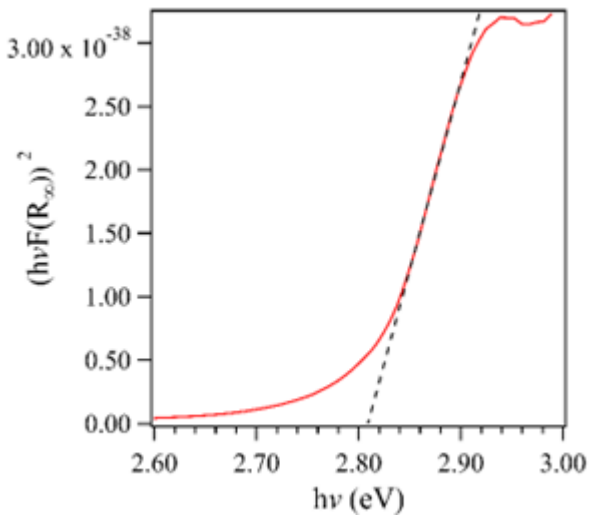


Figure S20. The Tauc's plot of $FA_4Pb_2Br_{7.5}(SCN)_{0.5}$ (x = 1). Band gap is estimated to 2.81 eV.

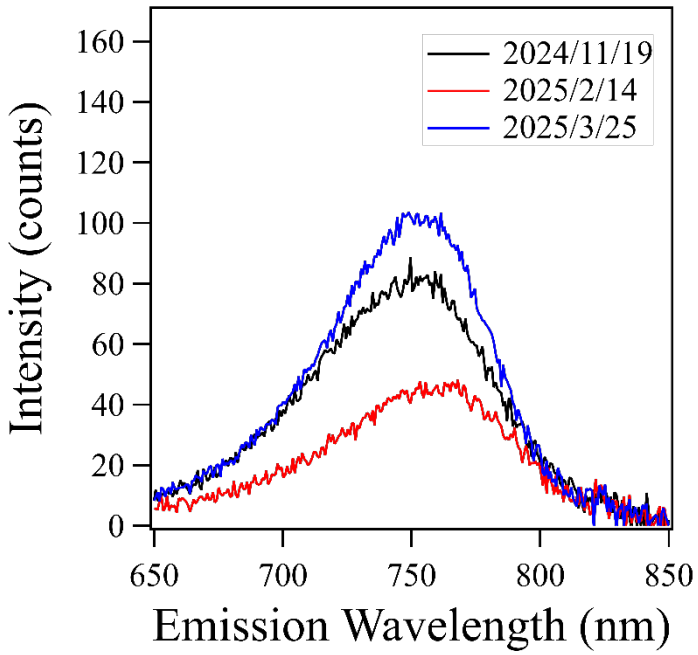


Figure S21. The result of absolute PL measurement for x = 0, the date represents the film fabrication date.

Table S4. Crystallographic data obtained by single crystal X-ray structure analysis. Estimated standard deviations are shown in parentheses.

Empirical formula	$C_8N_{16}Pb_4Br_{15.2}S_{0.8}$
Formula weight	2389.28
Temperature /K	293(2)
Crystal system	monoclinic
Space group	$P2_1/c$
a /Å	6.0372(3)
b /Å	25.564(2)
c /Å	8.6039(8)
α /°	90
β /°	94.902(6)
γ /°	90
Volume /Å^3	1323.05(19)
Z	1
ρ_{calc} g/cm^3	2.999
μ /mm^{-1}	24.219
F (0 0 0)	1033.0
Crystal size /mm^3	0.1 × 0.04 × 0.03
Radiation	Mo Kα (λ = 0.71073)
2θ range for data collection /°	4.752 to 52.738
Index ranges	$-7 \le h \le 5$, $-31 \le k \le 31$, $-10 \le l \le 10$
Reflections collected	13195
Independent reflections	2719 [R_{int} = 0.0391, R_{sigma} = 0.0323]
Data / Restraints / Parameters	2719 / 0 / 109
Goodness-of-fit on F^2	1.053
Final R indexes [$I \ge 2\sigma(I)$]	R_1 = 0.0415, wR_2 = 0.1031
Final R indexes [all data]	R_1 = 0.0577, wR_2 = 0.1102
Largest diff. peak / hole /e Å^{-3}	1.15 / −1.88

Table S5. Fractional atomic coordinates and equivalent isotropic displacement parameters (Å^2) obtained by single crystal X-ray structure analysis. U_{eq} is defined as 1/3 of the trace of the orthogonalized U_{IJ} tensor. Estimated standard deviations are shown in parentheses.

Atom	*x*	*y*	*z*	U_{eq} /Å^2	Occupancy
Pb01	0.43167(4)	3363.9(2)	5276.2(3)	0.04761(15)	1
Br02	0.39169(19)	0.41393(4)	0.27565(13)	0.0754(5)	0.951(7)
Br03	0.43216(16)	0.25000(4)	0.27963(11)	0.0810(3)	1
Br04	0.4617(2)	0.41783(4)	0.77229(14)	0.0903(6)	0.954(8)
Br05	0.93095(13)	0.33959(5)	0.53156(16)	0.0990(5)	1
N5	0.8440(30)	0.4798(6)	0.4580(20)	0.170(7)	1
N8	0.0340(50)	0.1820(13)	0.4560(30)	0.251(15)	1
C3	1	0.5	0.5	0.161(12)	1
N2	-0.1910(60)	0.1617(11)	0.6120(40)	0.286(18)	1
C4	-0.0800(40)	0.1775(10)	0.5370(30)	0.154(8)	1
N1	0.0450(30)	0.5301(12)	0.0740(40)	0.244(13)	1
C2	1570(140)	5030(20)	-0.0070(50)	0.200(30)	0.5
S02	0.39169(19)	0.41393(4)	0.27565(13)	0.0754(5)	0.049(7)
S04	0.4617(2)	0.41783(4)	0.77229(14)	0.0903(6)	0.046(8)

Table S6. Anisotropic displacement parameters (Å^2) obtained by single crystal X-ray structure analysis. The anisotropic displacement factor exponent takes the form: -2π2[h2a*2U11+2hka*b*U12+…]. Estimated standard deviations are shown in parentheses.

Atom	U_{11} /Å^2	U_{22} /Å^2	U_{33} /Å^2	U_{23} /Å^2	U_{13} /Å^2	U_{12} /Å^2
Pb01	0.03508(19)	0.0494(2)	0.0580(2)	0.00096(13)	0.00164(13)	0.00095(10)
Br02	0.0843(8)	0.0669(7)	0.073.(7)	0.0127(5)	-0.0018(5)	0.0055(4)
Br03	0.09.6(8)	0.0693(7)	0.0796(7)	-0.0182(5)	0.0041(6)	-0.0053(5)
Br04	0.1129(10)	0.0756(9)	0.0809(9)	-20.2(6)	0.0003(6)	0.0009(6)
Br05	0.0341(5)	0.1130(11)	0.1497(13)	0.0242(7)	0.0071(6)	0.0033(4)
N5	0.120(10)	0.154(11)	0.241(18)	-0.039(12)	0.038(12)	-0.068(10)
N8	0.270(30)	0.270(30)	0.230(30)	-0.001(19)	0.140(20)	-0.110(20)
C3	0.090(16)	0.250(40)	0.140(20)	-0.040(20)	0.032(15)	-0.020(20)
N2	0.290(30)	0.310(40)	0.290(30)	0.007(19)	0.220(30)	0.033(19)
C4	0.170(20)	0.120(15)	0.180(30)	0.005(14)	0.046(19)	0.002(12)
N1	0.107(14)	0.310(30)	0.310(30)	0.140(30)	-0.050(16)	-0.037(15)
C2	0.360(100)	0.130(30)	0.110(30)	0.050(20)	0.080(50)	0.070(50)

S02	0.0843(8)	0.0669(7)	0.0733(7)	0.0127(5)	-0.0018(5)	0.0055(4)
S04	0.1129(10)	0.0756(9)	0.0809(9)	-0.0202(6)	0.0003(6)	0.0009(6)

Table S7. Bond lengths obtained by single crystal X-ray structure analysis. Estimated standard deviations are shown in parentheses.

Atom	Atom	Length /Å
Pb01	Br02	2.9321(10)
Pb01	Br03[1]	3.0949(9)
Pb01	Br03	3.0711(9)
Pb01	Br04	2.9553(11)
Pb01	Br05	3.0127(8)
Pb01	Br05[2]	3.0271(8)
Pb01	S02	2.9321(10)
Pb01	S04	2.9553(11)
N5	C3	1.109(14)
N8	C4	1.03(3)
N2	C4	1.06(3)
N1	C2[3]	1.55(8)
N1	C2	1.23(4)
C2	C2[3]	1.91(16)

[1]+X,1/2-Y,1/2+Z; [2]-1+X,+Y,+Z; [3]-X,1-Y,-Z

Table S8. Bond angle obtained by single crystal X-ray structure analysis. Estimated standard deviations are shown in parentheses.

Atom	Atom	Atom	Angle /°	Atom	Atom	Atom	Angle /°
Br02	Pb01	Br03[1]	174.56(3)	Br05	Pb01	Br05[2]	176.65(5)
Br02	Pb01	Br03	88.70(3)	S02	Pb01	Br03	88.70(3)
Br02	Pb01	Br04	92.67(4)	S02	Pb01	Br05	90.52(3)
Br02	Pb01	Br05[2]	88.33(3)	S02	Pb01	S04	92.67(4)
Br02	Pb01	Br05	90.52(3)	S04	Pb01	Br03	176.27(3)
Br03	Pb01	Br03[1]	88.484(10)	S04	Pb01	Br05	88.42(4)
Br04	Pb01	Br03[1]	90.42(3)	Pb01	Br03	Pb01[3]	179.53(4)
Br04	Pb01	Br03	176.27(3)	Pb01	Br05	Pb01[4]	176.65(5)
Br04	Pb01	Br05[2]	88.49(4)	N5	C3	N5[5]	180
Br04	Pb01	Br05	88.42(4)	N8	C4	N2	164(4)

Br05	Pb01	Br03	88.11(3)	C2	N1	C2[6]	86(6)
Br05[2]	Pb01	Br03	95.02(3)	N1	C2	N1[6]	94(6)
Br05[2]	Pb01	Br03[1]	87.28(3)	N1	C2	C2[6]	54(3)
Br05	Pb01	Br03[1]	94.04(3)	N1[6]	C2	C2[6]	40(4)

[1]+X,1/2-Y,1/2+Z; [2]-1+X,+Y,+Z; [3]+X,1/2-Y,-1/2+Z; [4]1+X,+Y,+Z; [5]2-X,1-Y,1-Z; [6]-X,1-Y,-Z

Reference

1 T. Ohmi, J. R. Neilson, W. Taniguchi, T. Fukui, T. Nagase, Y. Haruta, M. I. Saidaminov, T. Fukushima, M. Azuma and T. Yamamoto, *ACS Mater Lett*, 2024, 6, 1913–1919.

2 S. A. Fateev, A. A. Petrov, E. I. Marchenko, Y. V. Zubavichus, V. N. Khrustalev, A. V. Petrov, S. M. Aksenov, E. A. Goodilin and A. B. Tarasov, *Chemistry of Materials*, 2021, 33, 1900–1907.